Journal of Sound and Vibration 329 (2010) 3382–3396

Contents lists available at ScienceDirect

Journal of Sound and Vibration

journal homepage: www.elsevier.com/locate/jsvi

Exact closed-form frequency equations for thick circular plates using a third-order shear deformation theory

Sh. Hosseini-Hashemi [a], M. Es'haghi [a], H. Rokni Damavandi Taher [b,*], M. Fadaie [a]

[a] *Impact Research Laboratory, School of Mechanical Engineering, Iran University of Science and Technology, Narmak, Tehran 16846-13114, Iran*
[b] *School of Engineering, University of British Columbia Okanagan, Kelowna, BC, Canada V1V 1V7*

ARTICLE INFO

Article history:
Received 8 July 2009
Received in revised form
18 February 2010
Accepted 19 February 2010
Handling Editor: S. Ilanko
Available online 19 March 2010

ABSTRACT

This paper presents, for the first time, exact closed-form frequency equations and transverse displacement for thick circular plates with free, soft simply supported, hard simply supported and clamped boundary conditions based on Reddy's third-order shear deformation theory. Hamiltonian and minimum potential energy principles are used to extract the equations of dynamic equilibrium and natural boundary conditions of the plate. The new formulation is verified by comparing the results with their counterparts reported in open literature. Natural frequencies of circular plates with different boundary conditions are tabulated in dimensionless form for various values of thickness–radius ratios. The results presented on the basis of exact, closed-form frequency equations are expected to serve as reliable benchmarks.

1. Introduction

Though there are several aspects of interest in the study of circular plates, free vibration analysis for obtaining natural frequencies plays a fundamental role in producing suitable designs of mechanical systems, from aerospace industry to microelectromechanical system (MEMS) devices.

A systematic summary of research studies on free vibration of circular plates made by Leissa [1], Weisensel [2] and Liew et al. [3] indicates that classical thin plate theory (CPT) and first-order shear deformation plate theory (FSDT) were mainly used by researchers. It is well known that CPT assumptions are satisfactory for low mode computation of thin plates and lead to inaccuracy in calculating higher modes. In fact, the CPT underestimates deflections and overestimates frequencies. In order to eliminate the above deficiency of the CPT, Deresiewicz and Mindlin [4] proposed the FSDT, including the effects of shear deformation and rotary inertia for moderately thick plates. Several papers were devoted to free vibration analysis of moderately thick circular plates. Rao and Prasad [5] presented the natural frequencies of circular plates on the basis of the FSDT. Liew et al. [6] developed the Mindlin solutions for flexural vibration of circular and annular plates with and without ring supports. Liew et al. [7] employed the differential quadrature method (DQM) to investigate axisymmetric free vibration analysis of circular Mindlin plates with different boundary conditions. Exact first two axisymmetric frequencies of circular Mindlin plates with different boundary conditions were presented by Irie et al. [8] using Bessel functions. Since the transverse shear strain is assumed to be constant through the thickness of the plate, a shear correction coefficient is needed in the FSDT to account for the prediction of uniform shear stress distribution. This coefficient depends on material properties, geometric dimensions and boundary conditions of the plate.

* Corresponding author. Tel.: +1 250 807 9652; fax: +1 250 807 8723.
E-mail address: hossein.rokni@ubc.ca (H. Rokni Damavandi Taher).

0022-460X/$ - see front matter
doi:10.1016/j.jsv.2010.02.024

Among various higher-order shear deformation plate theories (HSDT) [9–14], the third-order shear deformation theory of Reddy [13] is the most widely adopted model in the study of plates, especially laminated ones, due to its high efficiency and simplicity. The HSDT does not need to use any shear correction coefficient since its third-order displacement field assumption satisfies the zero shear stress condition at the free surfaces. Therefore, the HSDT, approximating radial and circumferential displacements up to the cubic order, produces better in-plane responses when compared with the FSDT. In return, their governing equations are much more complicated than those of the FSDT. Reddy and Phan [15] provided exact solutions for the free vibration and buckling of isotropic, orthotropic and laminated rectangular plates with simply supported edge condition according to the HSDT. Doong [16] employed the average stress method to present natural frequencies and buckling loads of simply supported rectangular plates on the basis of the HSDT. Hanna and Leissa [14] developed a completely HSDT to analyze free vibration of fully free rectangular plates using Rayleigh–Ritz method. Matsunaga [17] derived a HSDT through Hamilton's principle to investigate the stability and free vibration analysis of simply supported rectangular plates by Navier method. Wang et al. [18] derived an exact relationship between the natural frequencies of Reddy simply supported polygonal plates with those of the classical Kirchhoff ones. According to the FSDT and HSDT, Shufrin and Eisenberger [19] employed the extended Kantorovich method to present highly accurate numerical calculation of the natural frequencies and buckling loads for thick rectangular plates with various combinations of boundary conditions. Based on the FSDT and HSDT, an analysis of free vibrations of functionally graded rectangular plates with different boundary conditions was presented by Ferreira et al. [20] using the meshless method. There are few works on the free vibration of circular or annular plates on the basis of the HSDT. Chen and Hwang [21] utilized the average stress and Galerkin methods to obtain natural frequencies of axisymmetric initially stressed circular and annular plates using the HSDT. In addition, the finite element method based on the HSDT was used by Chen and Hwang [22] to study axisymmetric vibration and stability of thick annular plates under internal forces. Based on the HSDT, Hosseini-Hashemi et al. [23] provided an exact analytical solution for free vibration analysis of thick circular/annular plates, both upper and lower surfaces of which were in contact with a piezoelectric layer.

All researchers are willing to solve their plate problems exactly using the three-dimensional (3-D) elasticity theory in which no assumptions are made. However, due to the complex nature of the 3-D free vibration analysis of elastic plates, exact 3-D elasticity solutions were only yielded by Srinivas et al. [24] for simply supported rectangular plates and by Ding and Xu [25] for transversely isotropic circular plates under very limited boundary conditions. As a result, 3-D vibration analysis of circular plates with different boundary conditions must be carried out via numerical approaches, including the finite element method [26] and the Ritz method [27–32].

It is seen from the literature that exact solutions for vibratory characteristics of plates are available only for simple cases (i.e., a plate of usually rectangular shape with either simply supported boundary conditions based on the 3-D elasticity theory or different boundary conditions based on simplified theories such as the CPT and the FSDT) due to the mathematical and computational complexities.

The main objective of this paper is to present exact solutions to free vibration problem of circular thick plates on the basis of Reddy's higher-order plate theory. The exact closed-form characteristic equations along with displacement field are obtained for the first time in explicit forms for circular plates having free, soft simply supported, hard simply supported and clamped boundary conditions. The dynamic version of the principle of the virtual displacements, i.e. Hamilton's principle, is applied to derive the linear equilibrium equations of the plate. Utilizing the HSDT will exactly satisfy zero shear stress boundary conditions at the free surfaces. The merit and the high accuracy of the current exact approach are demonstrated by comparing the results of the present HSDT with those obtained by the DQM [7], the exact FSDT [8] and the 3-D elasticity theory [28] for different boundary conditions and plate parameters. Then, dimensionless natural frequencies of circular plates with different boundary conditions are given in tabular form for various values of the thickness–radius ratios.

2. Mathematical formulation

Consider an isotropic homogeneous thick circular plate of uniform thickness h and radius a. The plate geometry and dimensions are defined in an orthogonal cylindrical coordinate system (r,θ,z) to extract mathematical formulations. The origin of the coordinate system is taken at the center of the plate in the middle plane, as shown in Fig. 1.

2.1. Displacement field

Based on Reddy's third-order shear deformation plate theory [13], straight material lines normal to the plate mid-plane before deformation will no longer remain straight. Thus, the displacement components of an arbitrary point within the plate domain, designated by u, v and w, are expressed in general form as

$$u(r,\theta,z,t)=u_0(r,\theta,t)+z\psi_r(r,\theta,t)+z^2\varphi_r(r,\theta,t)+z^3\xi_r(r,\theta,t) \tag{1a}$$

$$v(r,\theta,z,t)=v_0(r,\theta,t)+z\psi_\theta(r,\theta,t)+z^2\varphi_\theta(r,\theta,t)+z^3\xi_\theta(r,\theta,t) \tag{1b}$$

$$w(r,\theta,z,t)=w_0(r,\theta,t) \tag{1c}$$

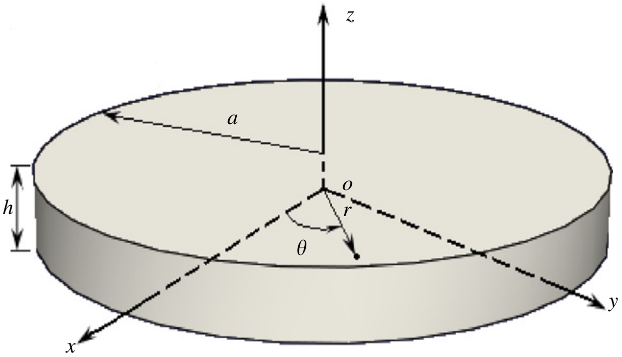

Fig. 1. Geometry and the coordinate system of a circular plate.

where u_0 and v_0 denote the in-plane displacements on mid-plane; w_0 is the transverse displacement; ψ_r and ψ_θ are the slope rotations in the $r-z$ and $\theta-z$ planes at z=0, respectively, φ_i and ξ_i (i=r,θ) are the higher-order displacement parameters defined at the mid-plane, and t is the time.

In this study, since the flexural vibration of the plate is studied, the in-plane displacements u_0 and v_0 are omitted. For simplicity, the notation w is used for w_0 in the following derivation of the governing equations of the plate. By satisfying zero shear stress boundary conditions at the top and bottom planes of the plate, the displacement field is then obtained as

$$u(r,\theta,z,t)=z\psi_r-\frac{4z^3}{3h^2}\left(\psi_r+\frac{\partial w}{\partial r}\right) \tag{2a}$$

$$v(r,\theta,z,t)=z\psi_\theta-\frac{4z^3}{3h^2}\left(\psi_\theta+\frac{\partial w}{r\partial\theta}\right) \tag{2b}$$

$$w(r,\theta,z,t)=W(r,\theta,t) \tag{2c}$$

2.2. Strain displacement relations

By neglecting the normal strain in the thickness direction ε_{zz}, the strains associated with the displacements in Eq. (2a)–(2c) are given for small deformation as

$$\varepsilon_{rr}=\frac{\partial u}{\partial r},\quad \varepsilon_{\theta\theta}=\frac{u}{r}+\frac{\partial v}{r\partial\theta},\quad \varepsilon_{zz}=0,\quad \varepsilon_{r\theta}=\frac{\partial v}{\partial r}+\frac{\partial u}{r\partial\theta}-\frac{v}{r},\quad \varepsilon_{rz}=\frac{\partial u}{\partial z}+\frac{\partial w}{\partial r},\quad \varepsilon_{\theta z}=\frac{\partial v}{\partial z}+\frac{\partial w}{r\partial\theta} \tag{3a–f}$$

where $\partial(\bullet)/\partial r$ ($\bullet$=u,v and w), for example, denotes the partial derivative with respect to r; ε_{rr} and $\varepsilon_{\theta\theta}$ are the normal strains and $\varepsilon_{r\theta}$, ε_{rz} and $\varepsilon_{\theta z}$ are the shear strains.

2.3. Hook's law

The stress–strain relations for the elastic plate can be written as

$$\sigma_r=\frac{E}{(1-v^2)}(\varepsilon_{rr}+v\varepsilon_{\theta\theta}),\quad \sigma_\theta=\frac{E}{(1-v^2)}(\varepsilon_{\theta\theta}+v\varepsilon_{rr}),\quad \sigma_{r\theta}=\frac{E}{2(1+v)}\varepsilon_{r\theta},\quad \sigma_{rz}=\frac{E}{2(1+v)}\varepsilon_{rz},\quad \sigma_{\theta z}=\frac{E}{2(1+v)}\varepsilon_{\theta z} \tag{4a–e}$$

where E and v are Young's modulus and Poisson's ratio, respectively.

2.4. Equations of motion

For free vibration, the kinetic energy T and the strain energy V of an elastic circular Reddy plate is expressed as

$$T=\frac{1}{2}\int_0^a\int_0^{2\pi}\int_{-h/2}^{h/2}\rho(\dot{u}^2+\dot{v}^2+\dot{w}^2)r\,dr\,d\theta\,dz \tag{5}$$

and

$$V=\frac{1}{2}\int_0^a\int_0^{2\pi}\int_{-h/2}^{h/2}(\sigma_r\varepsilon_{rr}+\sigma_\theta\varepsilon_{\theta\theta}+\sigma_{rz}\varepsilon_{rz}+\sigma_{\theta z}\varepsilon_{\theta z}+\sigma_{r\theta}\varepsilon_{r\theta})r\,dr\,d\theta\,dz \tag{6}$$

where ρ is the plate density and dot-overscript convention represents the differentiation with respect to the time variable t. After applying Hamilton's principle, three equations of motion for dynamic behavior of circular Reddy plates can be found as follows:

$$\frac{\partial M_r}{\partial r}+\frac{1}{r}\frac{\partial M_{r\theta}}{\partial \theta}-\frac{4}{3h^2}\left(\frac{\partial P_r}{\partial r}+\frac{1}{r}\frac{\partial P_{r\theta}}{\partial \theta}\right)+\frac{4}{3h^2}\frac{P_\theta-P_r}{r}+\frac{M_r-M_\theta}{r}+\frac{4}{h^2}R_r-Q_r=\bar{I}_3\ddot{\psi}_r-\frac{4}{3h^2}\bar{I}_5\frac{\partial \ddot{w}}{\partial r} \tag{7a}$$

$$\frac{\partial M_{r\theta}}{\partial r}+\frac{\partial M_\theta}{r\partial \theta}-\frac{4}{3h^2}\left(\frac{\partial P_{r\theta}}{\partial r}+\frac{1}{r}\frac{\partial P_\theta}{\partial \theta}\right)-\frac{8}{3h^2}\frac{P_{r\theta}}{r}+\frac{2M_{r\theta}}{r}+\frac{4}{h^2}R_\theta-Q_\theta=\bar{I}_3\ddot{\psi}_\theta-\frac{4}{3h^2}\bar{I}_5\frac{1}{r}\frac{\partial \ddot{w}}{\partial \theta} \tag{7b}$$

$$\begin{aligned}&\frac{\partial Q_r}{\partial r}+\frac{1}{r}\frac{\partial Q_\theta}{\partial \theta}-\frac{4}{h^2}\left(\frac{\partial R_r}{\partial r}+\frac{1}{r}\frac{\partial R_\theta}{\partial \theta}\right)+\frac{4}{3h^2}\left(\frac{\partial^2 P_r}{\partial r^2}+\frac{2}{r}\frac{\partial^2 P_{r\theta}}{\partial r\partial \theta}+\frac{1}{r^2}\frac{\partial^2 P_\theta}{\partial \theta^2}\right)+\frac{4}{3h^2}\left(\frac{2}{r}\frac{\partial P_r}{\partial r}-\frac{1}{r}\frac{\partial P_\theta}{\partial r}+\frac{2}{r^2}\frac{\partial P_{r\theta}}{\partial \theta}\right)\\&+\frac{1}{r}\left(Q_r-\frac{4}{h^2}R_r\right)=I_1\ddot{w}-\left(\frac{4}{3h^2}\right)^2 I_7\left(\frac{\partial^2 \ddot{w}}{\partial r^2}+\frac{1}{r}\frac{\partial \ddot{w}}{\partial r}+\frac{1}{r^2}\frac{\partial^2 \ddot{w}}{\partial \theta^2}\right)+\frac{4}{3h^2}\bar{I}_5\left(\frac{\partial \ddot{\psi}_r}{\partial r}+\frac{1}{r}\frac{\partial \ddot{\psi}_\theta}{\partial \theta}+\frac{\ddot{\psi}_r}{r}\right)\end{aligned} \tag{7c}$$

where the inertias I_i (i=1,2,3,4,5 and 7) are defined by

$$(I_1,I_2,I_3,I_4,I_5,I_7)=\int_{-h/2}^{h/2}\rho(1,z,z^2,z^3,z^4,z^6)\,dz \tag{8a}$$

$$\bar{I}_3=I_3-\frac{8}{3h^2}I_5+\frac{16}{9h^4}I_7 \tag{8b}$$

$$\bar{I}_5=I_5-\frac{4}{3h^2}I_7 \tag{8c}$$

and the expressions for bending moments M_r, M_θ, P_r, P_θ, twisting moments $M_{r\theta}$, $P_{r\theta}$ and shear forces Q_r, Q_θ, R_r, R_θ are

$$(M_i,P_i)=\int_{-h/2}^{h/2}\sigma_i(z,z^3)\,dz,\quad i=r,\theta \tag{9a}$$

$$(M_{r\theta},P_{r\theta})=\int_{-h/2}^{h/2}\sigma_{r\theta}(z,z^3)\,dz \tag{9b}$$

$$(Q_i,R_i)=\int_{-h/2}^{h/2}\sigma_{iz}(1,z^2)\,dz,\quad i=r,\theta \tag{9c}$$

2.5. Plate equations in dimensionless form

For generality and convenience in the mathematical formulation, the following dimensionless parameters are introduced:

$$R=\frac{r}{a},\quad Z=\frac{z}{h},\quad \Theta=\theta,\quad \delta=\frac{h}{a} \tag{10a–d}$$

For harmonic motion, the displacement field is taken as

$$\overline{u}(R,\Theta,Z)=\frac{1}{h}u(r,\theta,z,t)\,e^{-i\omega t} \tag{11a}$$

$$\overline{v}(R,\Theta,Z)=\frac{1}{h}v(r,\theta,z,t)\,e^{-i\omega t} \tag{11b}$$

$$\overline{w}(R,\Theta)=\frac{1}{a}w(r,\theta,t)\,e^{-i\omega t} \tag{11c}$$

where

$$\overline{u}(R,\Theta,Z)=Z\overline{\psi}_r-\frac{4}{3}Z^3\left(\overline{\psi}_r+\frac{\partial \overline{w}}{\partial R}\right) \tag{12a}$$

$$\overline{v}(R,\Theta,Z)=Z\overline{\psi}_\theta-\frac{4}{3}Z^3\left(\overline{\psi}_\theta+\frac{\partial \overline{w}}{R\partial \Theta}\right) \tag{12b}$$

$$\overline{w}(R,\Theta)=\overline{w} \tag{12c}$$

and $\overline{\psi}_j(R,\Theta)=\psi_j(r,\theta,t)\exp(-i\omega t)$ (j=r,θ).

Introducing the stress resultants in dimensionless form

$$\overline{M}_i=\frac{M_i}{Eh^2}\,e^{-i\omega t},\quad i=r,\theta,r\theta \tag{13a}$$

$$\overline{P}_i = \frac{P_i}{Eh^4}\, e^{-i\omega t}, \quad i = r, \theta, r\theta \tag{13b}$$

$$\overline{Q}_i = \frac{Q_i}{Eh}\, e^{-i\omega t}, \quad i = r, \theta \tag{13c}$$

$$\overline{R}_i = \frac{R_i}{Eh^3}\, e^{-i\omega t}, \quad i = r, \theta \tag{13d}$$

we have

$$(\overline{M}_r, \overline{P}_r) = \delta\left[(P_{11}, P_{21})\frac{\partial \overline{\psi}_r}{\partial R} + ((P_{11}-2A_{11}), (P_{21}-2A_{21}))\left(\frac{\partial \overline{\psi}_\theta}{R\partial \Theta} + \frac{\overline{\psi}_r}{R}\right) - (P_{12}, P_{22})\left(\frac{\partial^2 \overline{w}}{\partial R^2} + \frac{\partial \overline{w}}{R\partial R} + \frac{\partial^2 \overline{w}}{R^2 \partial \Theta^2}\right) + (P_{13}, P_{23})\frac{\partial^2 \overline{w}}{\partial R^2}\right] \tag{14a}$$

$$(\overline{M}_\theta, \overline{P}_\theta) = \delta\left[((P_{11}-2A_{11}), (P_{21}-2A_{21}))\frac{\partial \overline{\psi}_r}{\partial R} + (P_{11}, P_{21})\left(\frac{\partial \overline{\psi}_\theta}{R\partial \Theta} + \frac{\overline{\psi}_r}{R}\right) - (P_{14}, P_{24})\left(\frac{\partial^2 \overline{w}}{\partial R^2} + \frac{\partial \overline{w}}{R\partial R} + \frac{\partial^2 \overline{w}}{R^2 \partial \Theta^2}\right) - (P_{13}, P_{23})\frac{\partial^2 \overline{w}}{\partial R^2}\right] \tag{14b}$$

$$(\overline{M}_{r\theta}, \overline{P}_{r\theta}) = \delta\left[(A_{11}, A_{21})\left(\frac{\partial \overline{\psi}_r}{R\,\partial \Theta} + \frac{\partial \overline{\psi}_\theta}{\partial R} - \frac{\overline{\psi}_\theta}{R}\right) + (P_{13}, P_{23})\left(\frac{\partial^2 \overline{w}}{R\,\partial R\,\partial \Theta} - \frac{\partial \overline{w}}{R^2\,\partial \Theta}\right)\right] \tag{14c}$$

$$(\overline{Q}_r, \overline{R}_r) = (P_{15}, P_{25})\left(\overline{\psi}_r + \frac{\partial \overline{w}}{\partial R}\right) \tag{14d}$$

$$(\overline{Q}_\theta, \overline{R}_\theta) = (P_{15}, P_{25})\left(\overline{\psi}_\theta + \frac{\partial \overline{w}}{R\,\partial \Theta}\right) \tag{14e}$$

where

$$(\hat{I}_1, \hat{I}_2, \hat{I}_3, \hat{I}_4, \hat{I}_5, \hat{I}_7) = \int_{-1/2}^{1/2} (1, Z, Z^2, Z^3, Z^4, Z^6)\, dZ \tag{15a}$$

$$\tilde{I}_3 = \hat{I}_3 - \frac{8}{3}\hat{I}_5 + \frac{16}{9}\hat{I}_7 \tag{15b}$$

$$\tilde{I}_5 = \hat{I}_5 - \frac{4}{3}\hat{I}_7 \tag{15c}$$

$$P_{11} = \frac{1}{1-\nu^2}\left(\hat{I}_3 - \frac{4}{3}\hat{I}_5\right), \quad P_{12} = \frac{4}{3}\frac{\hat{I}_5 \nu}{1-\nu^2}, \quad P_{13} = -\frac{4}{3}\frac{\hat{I}_5}{(1+\nu)}, P_{14} = -\frac{4\hat{I}_5}{3(\nu^2-1)}, \quad P_{15} = \frac{1}{(1+\nu)}\left(\frac{\hat{I}_1}{2} - 2\hat{I}_3\right),$$
$$A_{11} = \frac{1}{2}(1-\nu)P_{11}, \quad P_{21} = \frac{1}{1-\nu^2}\left(\hat{I}_5 - \frac{4}{3}\hat{I}_7\right), \quad P_{22} = \frac{4}{3}\frac{\hat{I}_7 \nu}{1-\nu^2}, \quad P_{23} = -\frac{4}{3}\frac{\hat{I}_7}{(1+\nu)}, \quad P_{24} = -\frac{4\hat{I}_7}{3(\nu^2-1)},$$
$$P_{25} = \frac{1}{(1+\nu)}\left(\frac{\hat{I}_3}{2} - 2\hat{I}_5\right), \quad A_{21} = \frac{1}{2}(1-\nu)P_{21} \tag{15d−o}$$

Substituting Eqs. (14a)–(14e) into the moment and shear force resultants, Eqs. (13a)–(13d), and further into Eqs. (7a)–(7c) yields

$$\frac{12(1-\nu^2)}{\delta^4}\left(\delta\left(\frac{\partial \overline{M}_r}{\partial R} + \frac{1}{R}\frac{\partial \overline{M}_{r\theta}}{\partial \Theta} - \frac{4}{3}\left(\frac{\partial \overline{P}_r}{\partial R} + \frac{1}{R}\frac{\partial \overline{P}_{r\theta}}{\partial \Theta}\right) + \frac{4}{3}\frac{\overline{P}_\theta - \overline{P}_r}{R} + \frac{\overline{M}_r - \overline{M}_\theta}{R}\right) + 4\overline{R}_r - \overline{Q}_r\right) = -\tilde{I}_3 \beta^2 \overline{\psi}_r + \frac{4}{3}\tilde{I}_5 \beta^2 \frac{\partial \overline{w}}{\partial R} \tag{16a}$$

$$\frac{12(1-\nu^2)}{\delta^4}\left(\delta\left(\frac{\partial \overline{M}_{r\theta}}{\partial R} + \frac{\partial \overline{M}_\theta}{R\partial \Theta} - \frac{4}{3}\left(\frac{\partial \overline{P}_{r\theta}}{\partial R} + \frac{1}{R}\frac{\partial \overline{P}_\theta}{\partial \Theta}\right) - \frac{8}{3}\frac{\overline{P}_{r\theta}}{R} + \frac{2\overline{M}_{r\theta}}{R}\right) + 4\overline{R}_\theta - \overline{Q}_\theta\right) = -\tilde{I}_3 \beta^2 \overline{\psi}_\theta + \frac{4}{3}\tilde{I}_5 \beta^2 \frac{\partial \overline{w}}{R\partial \Theta} \tag{16b}$$

$$\frac{12(1-\nu^2)}{\delta^4}\left(\frac{\partial \overline{Q}_r}{\partial R} + \frac{1}{R}\,\frac{\partial \overline{Q}_\theta}{\partial \Theta} + \frac{1}{R}(\overline{Q}_r - 4\overline{R}_r) - 4\left(\frac{\partial \overline{R}_r}{\partial R} + \frac{1}{R}\,\frac{\partial \overline{R}_\theta}{\partial \Theta}\right) + \frac{4}{3}\delta\left(\frac{\partial^2 \overline{P}_r}{\partial R^2} + \frac{2}{R}\,\frac{\partial^2 \overline{P}_{r\theta}}{\partial R \partial \Theta} + \frac{1}{R^2}\frac{\partial^2 \overline{P}_\theta}{\partial \Theta^2}\right)\right.$$
$$\left. + \frac{4}{3}\delta\left(\frac{2}{R}\frac{\partial \overline{P}_r}{\partial R} - \frac{1}{R}\frac{\partial \overline{P}_\theta}{\partial R} + \frac{2}{R^2}\,\frac{\partial \overline{P}_{r\theta}}{\partial \Theta}\right)\right) = -\frac{\hat{I}_1}{\delta^2}\beta^2 \overline{w} + \frac{16}{9}\hat{I}_7 \beta^2\left(\frac{\partial^2 \overline{w}}{\partial R^2} + \frac{1}{R}\,\frac{\partial \overline{w}}{\partial R} + \frac{1}{R^2}\,\frac{\partial^2 \overline{w}}{\partial \Theta^2}\right) - \frac{4}{3}\tilde{I}_5 \beta^2\left(\frac{\partial \overline{\psi}_r}{\partial R} + \frac{1}{R}\frac{\partial \overline{\psi}_\theta}{\partial \Theta} + \frac{\overline{\psi}_r}{R}\right) \tag{16c}$$

where $\beta = \omega a^2 \sqrt{\rho h / D}$ is the frequency parameter in dimensionless form.

2.6. Solution for w, ψ_r and ψ_θ

Based on the Helmholtz decomposition, the rotations ψ_r and ψ_θ can be expressed in terms of the potential functions $\overline{R}(R,\Theta)$ and $\overline{H}(R,\Theta)$ as follows:

$$\overline{\psi}_r = \frac{\partial \overline{R}}{\partial R} + \frac{\partial \overline{H}}{R\,\partial \Theta} \tag{17a}$$

$$\overline{\psi}_\theta = \frac{\partial \overline{R}}{R\,\partial \Theta} - \frac{\partial \overline{H}}{\partial R} \tag{17b}$$

The solutions for $\overline{w}$, $\overline{R}$ and $\overline{H}$ in the Θ direction are assumed to take the following forms:

$$\overline{w}(R,\Theta) = \hat{w}(R)\cos(p\Theta) \tag{18a}$$

$$\overline{R}(R,\Theta) = \hat{R}(R)\cos(p\Theta) \tag{18b}$$

$$\overline{H}(R,\Theta) = \hat{H}(R)\sin(p\Theta) \tag{18c}$$

where the non-negative integer p represents the circumferential wavenumber of the corresponding mode shape. Substituting Eqs. (18a)–(18c) into the slope rotations, Eqs. (17a)–(17b), further into the moment and shear force resultants Eqs. (14a)–(14e), and then into Eqs. (16a)–(16c) yields

$$K_1\overline{\Delta}\overline{\Delta}\hat{R} - K_2\overline{\Delta}\hat{w} + \delta^2\left(K_3 + \frac{4}{3}\tilde{I}_5\beta^2\right)\overline{\Delta}\hat{R} + \delta^2\left(K_3 - \frac{16}{9}\hat{I}_7\beta^2\right)\overline{\Delta}\hat{w} + \hat{I}_1\beta^2\hat{w} = 0 \tag{19a}$$

$$\frac{\partial}{\partial R}\left[K_4\overline{\Delta}\hat{R} - \delta^2(K_3 - \tilde{I}_3\beta^2)\hat{R} - K_5\overline{\Delta}\hat{w} - \delta^2\left(K_3 + \frac{4}{3}\tilde{I}_5\beta^2\right)\hat{w}\right] + \frac{p}{R}[K_6\overline{\Delta}\hat{H} - \delta^2(K_3 - \tilde{I}_3\beta^2)\hat{H}] = 0 \tag{19b}$$

$$\frac{p}{R}\left[K_4\overline{\Delta}\hat{R} - \delta^2(K_3 - \tilde{I}_3\beta^2)\hat{R} - K_5\overline{\Delta}\hat{w} - \delta^2\left(K_3 + \frac{4}{3}\tilde{I}_5\beta^2\right)\hat{w}\right] + \frac{\partial}{\partial R}[K_6\overline{\Delta}\hat{H} - \delta^2(K_3 - \tilde{I}_3\beta^2)\hat{H}] = 0 \tag{19c}$$

The operator $\overline{\Delta}$ is defined as

$$\overline{\Delta} = \frac{\partial^2}{\partial R^2} + \frac{\partial}{R\partial R} - \frac{p^2}{R^2} \tag{20}$$

and

$$K_1 = -\frac{16}{3}(4\hat{I}_7 - 3\hat{I}_5),\quad K_2 = \frac{64}{3}\hat{I}_7,\quad K_3 = \frac{12(1-\nu)}{\delta^4}\left(\frac{\hat{I}_1}{2} - 4\hat{I}_3 + 8\hat{I}_5\right),\quad K_4 = 12\left(\hat{I}_3 - \frac{8}{3}\hat{I}_5 + \frac{16}{9}\hat{I}_7\right),$$
$$K_5 = 12\left(-\frac{16}{9}\hat{I}_7 + \frac{4}{3}\hat{I}_5\right),\quad K_6 = 6(1-\nu)\left(\hat{I}_3 - \frac{8}{3}\hat{I}_5 + \frac{16}{9}\hat{I}_7\right) \tag{21e–f}$$

In order to solve three complex coupled differential equations of motion, following steps must be taken so that Eqs. (19a)–(19c) become uncoupled:

1. Eq. (19b) is differentiated with respect to R.
2. Eq. (19b) divided by R.
3. Eq. (19c) is multiplied by $(-p/R)$.
4. If three equations obtained from steps (1)–(3) are added together, we will obtain
$$\overline{\Delta}\left[K_4\overline{\Delta}\hat{R} - \delta^2(K_3 - \tilde{I}_3\beta^2)\hat{R} - K_5\overline{\Delta}\hat{w} - \delta^2\left(K_3 + \frac{4}{3}\tilde{I}_5\beta^2\right)\hat{w}\right] = 0 \tag{22}$$
5. Eq. (19c) is differentiated with respect to R.
6. Eq. (19c) divided by R.
7. Eq. (19b) is multiplied by $(-p/R)$.
8. If three equations obtained from steps (5)–(7) are added together, we have
$$\overline{\Delta}[K_6\overline{\Delta}\hat{H} - \delta^2(K_3 - \tilde{I}_3\beta^2)\hat{H}] = 0 \tag{23}$$

In order to uncouple $\hat{R}$ and $\hat{w}$ in Eq. (22), transformation of variables is employed,

$$\hat{R} = x\hat{w} \tag{24}$$

where x is constant. Substituting Eq. (24) into Eq. (22) yields

$$\overline{\Delta}\left[\overline{\Delta}\hat{w}-\frac{\delta^2\left((K_3-\tilde{I}_3\beta^2)x+(K_3+(4/3)\tilde{I}_5\beta^2)\right)}{K_4x-K_5}\hat{w}\right]=0 \tag{25}$$

while substituting Eqs. (24) and (25) into Eq. (19a) yields

$$\overline{\Delta}\left[\overline{\Delta}\hat{w}-\frac{\delta^4\left((K_3+(4/3)\tilde{I}_5\beta^2)x+(K_3-(16/9)\hat{I}_7\beta^2)\right)\left((K_3-\tilde{I}_3\beta^2)x+(K_3+(4/3)\tilde{I}_5\beta^2)\right)+\hat{I}_1\beta^2(K_4x-K_5)}{\delta^2(K_2-K_1x)\left((K_3-\tilde{I}_3\beta^2)x+(K_3+(4/3)\tilde{I}_5\beta^2)\right)}\hat{w}\right]=0 \tag{26}$$

It is observed that the terms within the brackets in Eqs. (25) and (26) have an identical form. Thus, the solution for $\hat{w}$ will be unique provided that

$$\frac{\delta^2\left((K_3-\tilde{I}_3\beta^2)x+(K_3+(4/3)\tilde{I}_5\beta^2)\right)}{K_4x-K_5}=\frac{\delta^4\left(\left(K_3+(4/3)\tilde{I}_5\beta^2\right)x+(K_3-(16/9)\hat{I}_7\beta^2)\right)\left((K_3-\tilde{I}_3\beta^2)x+(K_3+(4/3)\tilde{I}_5\beta^2)\right)+\hat{I}_1\beta^2(K_4x-K_5)}{\delta^2(K_2-K_1x)\left((K_3-\tilde{I}_3\beta^2)x+(K_3+(4/3)\tilde{I}_5\beta^2)\right)} \tag{27}$$

Simplifying Eq. (27) yields a cubic equation which it has three roots x_1, x_2 and x_3. Thus, Eq. (25) can be reduced to

$$\overline{\Delta}\hat{w}-\lambda\hat{w}=0 \tag{28}$$

where

$$\lambda=\frac{\delta^2\left((K_3-\tilde{I}_3\beta^2)x+(K_3+(4/3)\tilde{I}_5\beta^2)\right)}{K_4x-K_5} \tag{29}$$

$\lambda_i(i=1,2,3)$ can be computed using three roots x_1, x_2 and x_3 getting from Eq. (27). Three Bessel functions $c_iw_{i1}(p,\chi_ir)$, $i=1,2,3$, where $\chi_i=\sqrt{|\lambda_i|}$ are obtained by substituting $\lambda_i(i=1,2,3)$ into Eq. (28). $c_i(i=1,2,3)$ are constants. Final solution can be given by

$$\hat{w}(R)=\sum_{i=1}^{3}c_iw_{i1}(p,\chi_iR) \tag{30a}$$

$$\hat{R}(R)=\sum_{i=1}^{3}x_i[c_iw_{i1}(p,\chi_iR)] \tag{30b}$$

where

$$w_{i1}(p,\chi_iR)=\begin{cases}J_p(\chi_iR), & \lambda_i<0,\\ I_p(\chi_iR), & \lambda_i>0,\end{cases}\quad i=1,2,3 \tag{31}$$

Substituting Eq. (25) into Eqs. (19b) and (19c) gives the following Bessel equation

$$\overline{\Delta}\hat{H}-\lambda_4\hat{H}=0 \tag{32}$$

where

$$\lambda_4=\frac{\delta^2(K_3-\tilde{I}_3\beta^2)}{K_6} \tag{33}$$

Finally, $\hat{H}$ can be expressed as

$$\hat{H}(R)=c_4w_{41}(p,\chi_4R) \tag{34}$$

in which

$$\chi_4=\sqrt{\lambda_4} \tag{35a}$$

$$w_{41}(p,\chi_4R)=\begin{cases}J_p(\chi_4R), & \lambda_i<0\\ I_p(\chi_4R), & \lambda_i>0\end{cases} \tag{35b}$$

and c_4 is constant. Substituting Eqs. (30) and (34) into Eqs. (18a)–(18c) and then into (17a)–(17b) gives

$$\overline{\psi}_r=\left[\sum_{i=1}^{3}x_i\left(c_i\frac{\partial w_{i1}}{\partial R}\right)+\frac{p}{R}c_4w_{41}\right]\cos(p\Theta) \tag{36a}$$

$$\overline{\psi}_\theta = -\left[\frac{p}{R}\sum_{i=1}^{3} x_i(c_i w_{i1}) + c_4\frac{\partial w_{41}}{\partial R}\right]\sin(p\Theta) \tag{36b}$$

2.7. Classical boundary conditions

The transverse displacement $\overline{w}$ along with the slope rotations $\overline{\psi}_r$ and $\overline{\psi}_\theta$ were exactly determined in terms of the frequency parameter β. Edge of the circular plate may take any classical boundary conditions, including free, soft simply supported, hard simply supported and clamped.

The boundary conditions at the edge of the circular plate is as follows:

- for a free edge

$$\overline{M}_r(R,\Theta)=0,\quad \overline{P}_r(R,\Theta)=0,\quad \overline{M}_{r\theta}-\frac{4}{3}\overline{P}_{r\theta}=0$$
$$\frac{12(1-v^2)}{\delta^4}\left(\overline{Q}_r-4\overline{R}_r+\frac{4}{3}\delta\frac{\partial\overline{P}_r}{\partial R}+\frac{4}{3}\delta\frac{\overline{P}_r-\overline{P}_\theta}{R}+\frac{8}{3}\delta\frac{1}{R}\frac{\partial\overline{P}_{r\theta}}{\partial\Theta}\right)+\frac{4}{3}\tilde{I}_5\beta^2\overline{\psi}_r-\frac{16}{9}\hat{I}_7\beta^2\frac{\partial\overline{w}}{\partial R}=0 \tag{37a–d}$$

- for a soft simply supported edge

$$\overline{w}(R,\Theta)=0,\quad \overline{M}_{r\theta}-\frac{4}{3}\overline{P}_{r\theta}=0,\quad \overline{M}_r(R,\Theta)=0,\quad \overline{P}_r(R,\Theta)=0 \tag{38a–d}$$

- for a hard simply supported edge

$$\overline{w}(R,\Theta)=0,\quad \overline{\psi}_\theta(R,\Theta)=0,\quad \overline{M}_r(R,\Theta)=0,\quad \overline{P}_r(R,\Theta)=0 \tag{39a–d}$$

- for a clamped edge

$$\overline{w}(R,\Theta)=0,\quad \frac{\partial}{\partial R}[\overline{w}(R,\Theta)]=0,\quad \overline{\psi}_r(R,\Theta)=0,\quad \overline{\psi}_\theta(R,\Theta)=0 \tag{40a–d}$$

Natural frequencies of circular plates in dimensionless form ($\beta=\omega a^2\sqrt{\rho h/D}$) can be calculated by using above boundary conditions. Exact closed-form characteristic equations of circular plates under different boundary conditions are given in detail in Appendix A.

3. Results and discussion

Based on Reddy's higher-order plate theory, a computer code was developed to obtain exact natural frequencies of free flexural vibration of circular plates with free, soft simply supported, hard simply supported and clamped boundary conditions while various values of the thickness to radius ratios were used. All frequencies are expressed in terms of the dimensionless parameter $\beta=\omega a^2\sqrt{\rho h/D}$. For all calculations here, Poisson's ratio v has been taken as 0.3. The numbers in parentheses (p, s) show that the vibrating mode has p nodal diameters and vibrates in the sth mode for the given p value.

A code was developed for the solution of the associated eigenvalue problem.

Table 1
Comparison of frequency parameters β of circular plates under different boundary conditions with those obtained by exact Mindlin plate theory [8].

Boundary conditions	(p, s)	δ=0.001			δ=0.25		
		HSDT	FSDT [8]	%Diff	HSDT	FSDT [8]	%Diff
Free	(0, 0)	9.00305	9.003	0.00	8.27233	8.267	0.06
	(0, 1)	38.4429	38.443	0.00	28.6931	28.605	0.31
	(0, 2)	87.7488	87.750	0.00	52.9333	52.584	0.66
	(0, 3)	156.814	156.818	0.00	77.7821	76.936	1.09
Simply supported	(0, 0)	4.93536	4.935	0.00	4.69853	4.696	0.05
	(0, 1)	29.7199	29.720	0.00	23.3190	23.254	0.28
	(0, 2)	74.1551	74.156	0.00	47.0716	46.775	0.63
	(0, 3)	138.315	138.318	0.00	72.4038	71.603	1.11
Clamped	(0, 0)	10.2157	10.216	0.00	8.84637	8.807	0.44
	(0, 1)	39.7708	39.771	0.00	27.6223	27.253	1.34
	(0, 2)	89.1024	89.104	0.00	50.4941	49.420	2.13
	(0, 3)	158.179	158.184	0.00	75.1309	73.054	2.76

Table 2
Comparison of frequency parameters β of free circular plates with those obtained by the DQM [7].

δ	Method	Mode number (p, s)						
		(0,0)	(0,1)	(0,2)	(0,3)	(0,4)	(0,5)	(0,6)
0.001	HSDT	9.00305	38.4429	87.7488	156.814	245.622	354.169	482.449
	DQM [7]	9.0031	38.443	87.749	156.81	245.62	354.17	482.45
	%Diff	0.00	0.00	0.00	0.00	0.00	0.00	0.00
0.050	HSDT	8.96879	37.7930	84.473	146.852	222.598	309.411	405.201
	DQM [7]	8.9686	37.787	84.443	146.76	222.38	308.98	404.44
	%Diff	0.00	0.02	0.03	0.06	0.10	0.14	0.19
0.100	HSDT	8.86880	36.0613	76.7776	126.564	182.092	241.141	302.296
	DQM [7]	8.8679	36.041	76.676	126.27	181.46	239.98	300.38
	%Diff	0.01	0.06	0.13	0.23	0.35	0.48	0.63
0.150	HSDT	8.71147	33.7157	68.0103	106.895	147.866	189.621	231.272
	DQM [7]	8.7095	33.674	67.827	106.40	146.83	187.79	228.39
	%Diff	0.02	0.12	0.27	0.46	0.70	0.97	1.25
0.200	HSDT	8.50842	31.1748	59.9152	90.7511	121.931	151.773	172.673
	DQM [7]	8.5051	31.111	59.645	90.645	120.57	149.63	171.18
	%Diff	0.04	0.20	0.45	0.12	1.12	1.41	0.87
0.250	HSDT	8.27233	28.6931	52.9333	77.7821	100.944	115.596	127.963
	DQM [7]	8.2674	28.605	52.584	76.936	99.545	114.53	126.34
	%Diff	0.06	0.31	0.66	1.09	1.39	0.92	1.27

Table 3
Comparison of frequency parameters β of hard simply supported circular plates with those obtained by the DQM [7].

δ	Method	Mode number (p, s)						
		(0,0)	(0,1)	(0,2)	(0,3)	(0,4)	(0,5)	(0,6)
0.001	HSDT	4.93536	29.7199	74.1551	138.315	222.206	325.830	449.184
	DQM [7]	4.9351	29.720	74.155	138.31	222.21	325.83	449.18
	%Diff	0.00	0.00	0.00	0.00	0.00	0.00	0.00
0.050	HSDT	4.92479	29.3272	71.7804	130.429	203.000	287.179	380.823
	DQM [7]	4.9247	29.323	71.756	130.35	202.81	286.79	380.13
	%Diff	0.00	0.01	0.03	0.06	0.09	0.13	0.18
0.100	HSDT	4.89421	28.2547	66.0243	113.823	168.091	226.401	287.219
	DQM [7]	4.8938	28.240	65.942	113.57	167.53	225.34	285.44
	%Diff	0.01	0.05	0.12	0.22	0.33	0.47	0.62
0.150	HSDT	4.84480	26.7445	59.2143	97.2093	137.915	179.958	222.705
	DQM [7]	4.8440	26.715	59.062	96.775	136.98	178.23	219.86
	%Diff	0.02	0.11	0.26	0.45	0.68	0.96	1.28
0.200	HSDT	4.77871	25.0414	52.7387	83.3847	115.184	147.500	166.383
	DQM [7]	4.7773	24.994	52.514	82.766	113.87	145.13	166.29
	%Diff	0.03	0.19	0.43	0.74	1.14	1.61	0.056
0.250	HSDT	4.69853	23.3190	47.0716	72.4038	98.2801	108.326	124.499
	DQM [7]	4.6963	23.254	46.775	71.603	96.609	108.27	121.50
	%Diff	0.05	0.28	0.63	1.11	1.70	0.05	2.41

3.1. Verification of the present formulations

In this subsection, three illustrative examples are presented in the following to demonstrate the high accuracy of the current exact solution procedure. The percentage difference given in Tables 1–5 is defined as follows:

$$\%\,\mathrm{Diff} = \frac{[(\text{Exact HSDT})-(\text{Other methods})]}{(\text{Exact HSDT})} \times 100$$

Example 1. Frequency parameters of circular plates under free, hard simply supported and clamped boundary conditions are presented in Table 1 for two values of the thickness to radius ratios δ=0.001 and 0.25. It should be noted that the exact results reported by Irie et al. [8] were based on the FSDT. It is seen from Table 1 that both theories yield identical results for

Table 4
Comparison of frequency parameters β of clamped circular plates with those obtained by the DQM [7].

δ	Method	Mode number (p, s)						
		(0,0)	(0,1)	(0,2)	(0,3)	(0,4)	(0,5)	(0,6)
0.001	HSDT	10.2157	39.7708	89.1024	158.179	246.994	355.543	483.825
	DQM [7]	10.216	39.771	89.102	158.18	246.99	355.54	483.82
	%Diff	0.00	0.00	0.00	0.00	0.00	0.00	0.00
0.050	HSDT	10.1459	38.8706	85.0647	146.601	221.173	306.548	400.72
	DQM [7]	10.145	38.855	84.995	146.40	220.73	305.71	399.32
	%Diff	0.01	0.04	0.08	0.14	0.20	0.27	0.35
0.100	HSDT	9.94614	36.5489	75.954	124.057	177.862	235.388	295.369
	DQM [7]	9.9408	36.479	75.664	123.32	176.41	232.97	291.71
	%Diff	0.05	0.19	0.38	0.59	0.82	1.03	1.24
0.150	HSDT	9.64191	33.5525	66.129	103.395	143.253	184.600	226.836
	DQM [7]	9.6286	33.393	65.551	102.09	140.93	180.99	221.62
	%Diff	0.14	0.47	0.87	1.26	1.62	1.96	2.30
0.200	HSDT	9.26503	30.4749	57.533	87.3224	118.491	150.371	176.378
	DQM [7]	9.2400	30.211	56.682	85.571	115.55	145.94	174.97
	%Diff	0.27	0.87	1.48	2.01	2.48	2.95	0.80
0.250	HSDT	8.84637	27.6223	50.4941	75.1309	100.568	118.332	127.098
	DQM [7]	8.8068	27.253	49.420	73.054	97.198	117.90	122.43
	%Diff	0.45	1.34	2.13	2.76	3.35	0.37	3.67

thin circular plates. However, the difference between two exact solutions increases for thicker plates with higher degrees of edge constraint, particularly at the higher modes of vibration. This is due to the fact that the Mindlin model cannot capture the boundary layer term for the clamped edge, while the higher-order shear deformation theories can do a much better job [33]. Furthermore, unlike the FSDT, the HSDT not only requires no shear correction factor but also models a plate with smaller displacements and higher rigidity. It is worth noting that all results obtained on the basis of the HSDT are greater than those of the FSDT.

Example 2. The first seven non-dimensional frequency parameters β of circular plates subjected to free, hard simply supported and clamped boundary conditions are presented in Tables 2–4 for a wide range of thickness to radius ratios from δ=0.001 to 0.25. The present exact results are found to be in good agreement with those reported by Liew et al. [7] using the DQM based on the FSDT. Note that observations in Tables 2–4 are similar to those in Table 1. In other words, the discrepancy becomes more significant with an increase in the thickness–radius ratio, wavenumber and boundary constraints.

Example 3. Table 5 exhibits the comparison of the frequency parameters β of circular plates with free, soft simply supported, hard simply supported and clamped boundary conditions for various values of thickness–radius ratios (δ=0.01, 0.1, 0.2 and 0.3) with those obtained using the Ritz 3-D method by Liew and Yang [28]. The discrepancy between the results of these two methods is very small and does not exceed 0.94% for the worst case. It can obviously be seen that all present results are smaller than those obtained by the Ritz 3-D solution. This is due to the fact that natural frequencies by the Ritz method are upper bounds of the exact ones, unless an exact eigenfunction of free vibration for the trial function is assumed.

3.2. Benchmark data

According to the above verification of the current approach, the authors have gained a strong position to give benchmark frequency results for comparisons with those from other methods. Exact natural frequency parameters of circular thin, moderately thick and thick plates under different classical boundary conditions are presented in Tables 6–9 for a large spectrum of values of thickness–radius ratios, varying from 0.01 to 0.35. The results are tabulated for three circumferential wavenumbers (p=0, 1, 2 and 3) while the first three modes (s=0 and 1) are considered for each value of p. It is seen from Tables 6–9 that the frequency parameters β decrease with an increase in the thickness–radius ratio δ. Such behavior is due to the influence of rotary inertia and shear deformations. It can also be observed that the frequency parameters β decrease when less restraining boundary is used at the edge of the plate. This is attributed to the fact that higher constraints at the edges increase the flexural rigidity of the plate, leading to a higher frequency response.

Table 5
Comparison of frequency parameters β of circular plates under different boundary conditions with those obtained by 3-D Ritz solution [28].

δ	Method	Mode number (p, s)				
		(0,0)	(0,1)	(1,0)	(2,0)	(3,0)
(a) Free circular plates						
0.01	HSDT	9.00175	38.4164	20.4613	5.35455	12.4238
	3D Ritz [28]	9.0018	38.417	20.466	5.3570	12.433
	%Diff	0.00	0.00	−0.02	−0.05	−0.07
0.1	HSDT	8.8688	36.0613	19.7172	5.27842	12.0675
	3D Ritz [28]	8.8720	36.132	19.738	5.2795	12.074
	%Diff	−0.04	−0.20	−0.10	−0.02	−0.05
0.2	HSDT	8.50842	31.1748	17.9983	5.11607	11.3233
	3D Ritz [28]	8.5194	–	18.056	5.1185	11.337
	%Diff	−0.13	–	−0.32	−0.05	−0.12
0.3	HSDT	8.01507	26.3883	16.0153	4.89609	10.4176
	3D Ritz [28]	8.0344	–	16.102	4.9005	10.439
	%Diff	−0.24	–	−0.54	−0.09	−0.20
(b) Soft simply supported circular plates						
0.01	HSDT	4.93473	29.7039	13.8892	25.5805	39.8828
	3D Ritz [28]	4.9360	29.706	13.894	25.597	39.918
	%Diff	−0.03	−0.01	−0.035	−0.06	−0.09
0.1	HSDT	4.89421	28.2547	13.5142	24.3263	36.9926
	3D Ritz [28]	4.8975	28.310	13.529	24.371	37.091
	%Diff	−0.07	−0.20	−0.11	−0.18	−0.27
0.2	HSDT	4.77871	25.0414	12.6324	21.7279	31.6336
	3D Ritz [28]	4.7876	25.188	12.677	21.845	31.859
	%Diff	−0.19	−0.589	−0.359	−0.54	−0.71
0.3	HSDT	4.60704	21.6757	11.5435	18.9731	26.6333
	3D Ritz [28]	4.6234	21.879	11.618	19.142	–
	%Diff	−0.35	−0.94	−0.64	−0.89	–
(c) Hard simply supported circular plates						
0.01	HSDT	4.93473	29.7039	13.8947	25.6014	39.9281
	3D Ritz [28]	4.9360	29.706	13.896	25.603	39.930
	%Diff	−0.03	−0.01	−0.01	−0.01	0.00
0.1	HSDT	4.89421	28.2547	13.5657	24.5128	37.3785
	3D Ritz [28]	4.8975	28.310	13.580	24.555	37.472
	%Diff	−0.07	−0.20	−0.10	−0.17	−0.25
0.2	HSDT	4.77871	25.0414	12.7196	22.0128	32.1626
	3D Ritz [28]	4.7876	25.188	12.764	22.130	32.389
	%Diff	−0.19	−0.58	−0.35	−0.53	−0.70
0.3	HSDT	4.60704	21.6757	11.6491	19.2838	27.1569
	3D Ritz [28]	4.6234	21.879	11.723	19.453	–
	%Diff	−0.35	−0.94	−0.63	−0.88	–
(d) Clamped circular plates						
0.01	HSDT	10.2130	39.7336	21.2487	34.8467	50.9670
	3D Ritz [28]	10.250	39.878	21.326	34.974	51.155
	%Diff	−0.36	−0.36	−0.36	−0.36	−0.37
0.1	HSDT	9.94614	36.5489	20.1993	32.2634	45.8905
	3D Ritz [28]	9.9909	36.744	20.297	32.430	46.140
	%Diff	−0.45	−0.53	−0.48	−0.52	−0.54
0.2	HSDT	9.26503	30.4749	17.8550	27.2148	37.1513
	3D Ritz [28]	9.3225	30.649	17.963	27.366	37.338
	%Diff	−0.62	−0.57	−0.60	−0.56	−0.50
0.3	HSDT	8.4113	25.1011	15.3850	22.6165	30.0729
	3D Ritz [28]	8.4676	25.150	15.453	22.667	30.093
	%Diff	−0.67	−0.19	−0.44	−0.22	−0.07

4. Concluding remarks

In this paper, exact closed-form solutions were presented to investigate free vibration behavior of circular plates under free, soft simply supported, hard simply supported and clamped boundary conditions based on Reddy's third-order shear deformation plate theory. Governing equations for freely vibrating circular plates were derived by applying Hamilton's principle. The exact closed-form characteristic equations along with the transverse displacement were presented for circular plates with all classical boundary conditions. The accuracy of the current solution was verified by comparing the

Table 6
Frequency parameters β of free circular plates with different thickness to radius ratios.

δ	Mode number (p, s)							
	(0,0)	(0,1)	(1,0)	(1,1)	(2,0)	(2,1)	(3,0)	(3,1)
0.01	9.00175	38.4164	20.4613	59.7396	5.35449	35.2141	12.4237	52.9044
0.05	8.96879	37.7930	20.2618	58.2289	5.32987	34.6044	12.3120	51.5505
0.10	8.86880	36.0613	19.7172	54.3066	5.27842	33.0529	12.0675	48.2702
0.15	8.71147	33.7157	18.9292	49.4351	5.20616	30.9798	11.7286	44.1964
0.20	8.50842	31.1748	17.9983	44.5751	5.11607	28.7256	11.3233	40.0783
0.25	8.27233	28.6931	17.0078	40.1354	5.01154	26.5048	10.8788	36.2652
0.30	8.01507	26.3883	16.0153	36.2100	4.89609	24.4214	10.4176	32.8598
0.35	7.74669	24.2979	15.0543	32.7549	4.77299	22.5107	9.9562	29.8517

Table 7
Frequency parameters β of soft simply supported circular plates with different thickness to radius ratios.

δ	Mode number (p, s)							
	(0,0)	(0,1)	(1,0)	(1,1)	(2,0)	(2,1)	(3,0)	(3,1)
0.01	4.93474	29.7039	13.8892	48.4311	25.5805	70.0078	39.8828	94.3424
0.05	4.92479	29.3272	13.7851	47.4220	25.2197	67.8979	39.0327	90.5505
0.10	4.89421	28.2547	13.5142	44.7285	24.3263	62.6278	36.9926	81.6577
0.15	4.84480	26.7445	13.1169	41.2471	23.1045	56.3531	34.3771	71.8455
0.20	4.77871	25.0414	12.6324	37.6477	21.7279	50.3339	31.6336	63.0152
0.25	4.69853	23.3190	12.0979	34.2762	20.3250	45.0250	29.0164	55.5912
0.30	4.60704	21.6757	11.5435	31.2578	18.9731	40.4885	26.6333	49.4677
0.35	4.50697	20.1569	10.9909	28.6087	17.7109	36.6465	24.5111	44.4149

Table 8
Frequency parameters β of hard simply supported circular plates with different thickness to radius ratios.

δ	Mode number (p, s)							
	(0,0)	(0,1)	(1,0)	(1,1)	(2,0)	(2,1)	(3,0)	(3,1)
0.01	4.93474	29.7039	13.8947	48.4359	25.6014	70.0270	39.9281	94.3852
0.05	4.92479	29.3272	13.8122	47.4451	25.3209	67.9868	39.2510	90.7438
0.10	4.89421	28.2547	13.5657	44.7685	24.5128	62.7737	37.3785	81.9578
0.15	4.84480	26.7445	13.1886	41.2965	23.3519	56.5240	34.8624	72.1795
0.20	4.77871	25.0414	12.7196	37.7014	22.0128	50.5116	32.1626	63.3481
0.25	4.69853	23.3190	12.1962	34.3314	20.6291	45.2019	29.5530	55.9130
0.30	4.60704	21.6757	11.6491	31.3134	19.2838	40.6630	27.1569	49.7802
0.35	4.50697	20.1569	11.1008	28.6645	18.0201	36.8213	25.0113	44.7274

Table 9
Frequency parameters β of clamped circular plates with different thickness to radius ratios.

δ	Mode number (p, s)							
	(0,0)	(0,1)	(1,0)	(1,1)	(2,0)	(2,1)	(3,0)	(3,1)
0.01	10.2130	39.7336	21.2487	60.7438	34.8467	84.4223	50.9670	110.750
0.05	10.1459	38.8706	20.9760	58.8329	34.1503	80.8872	49.5448	104.900
0.10	9.94614	36.5489	20.1993	53.9980	32.2634	72.4899	45.8905	91.8557
0.15	9.64191	33.5525	19.1006	48.2816	29.7933	63.3388	41.4558	78.6631
0.20	9.26503	30.4749	17.8550	42.8755	27.2148	55.2584	37.1513	67.6580
0.25	8.84637	27.6223	16.5911	38.1773	24.7887	48.5935	33.3357	58.9236
0.30	8.41130	25.1011	15.3850	34.2466	22.6165	43.1844	30.0729	52.0154
0.35	7.97828	22.9183	14.2728	30.9574	20.7150	38.7781	27.3141	46.4874

present frequency parameters with those available in the literature. Although both FSDT and HSDT solutions acquired the same frequency parameters for thin circular plates, the discrepancy increased for thicker plates with higher degrees of edge constraint, especially at the higher modes of vibration. It was also seen that as compared to the DQM solution of Liew et al. [7] and the FSDT solution of Irie et al. [8], the proposed HSDT method was closer to the 3-D elasticity solution of Liew and Yang [28]. In order to examine the correctness of other analytical and numerical methods given in the future, exact vibration frequencies of circular thin, moderately thick and thick plates with different boundary conditions were tabulated to serve as the benchmark data.

Appendix A. Exact closed-form characteristic equations

There exist closed-form exact solutions to the characteristic equations of circular plates under free, soft simply supported, hard simply supported and clamped boundary conditions. After expanding the determinant and performing mathematical manipulations, exact characteristic equations can be listed below for each individual case.

Case 1: Clamped circular plates

$$-x_1(L_3(1)w_{21}(1)-L_2(1)w_{31}(1))(L_1(1)L_4(1)-p^2w_{11}(1)w_{41}(1))+x_2(L_3(1)w_{11}(1)-L_1(1)w_{31}(1))(L_2(1)L_4(1)-p^2w_{21}(1)w_{41}(1))-x_3(L_2(1)w_{11}(1)-L_1(1)w_{21}(1))(L_3(1)L_4(1)-p^2w_{31}(1)w_{41}(1))=0 \tag{A.1}$$

where

$$w_{i1}(R)=w_{i1}(p,\chi_iR), \quad L_i(R)=\frac{\partial}{\partial R}w_{i1}(p,\chi_iR), \quad i=1,2,3,4 \tag{A.2,3}$$

Case 2: Hard simply supported circular plates

$$L_4(1)\Big((-\alpha_3\Lambda_2+\alpha_2\Lambda_3)w_{11}(1)+(\alpha_3\Lambda_1-\alpha_1\Lambda_3)w_{21}(1)+(-\alpha_2\Lambda_1+\alpha_1\Lambda_2)w_{31}(1)\Big)+p\Big((x_2-x_3)(\alpha_4\Lambda_1-\alpha_1\Lambda_4)w_{21}(1)w_{31}(1)+w_{11}(1)\Big((x_1-x_2)(\alpha_4\Lambda_3-\alpha_3\Lambda_4)w_{21}(1)-(x_1-x_3)(\alpha_4\Lambda_2-\alpha_2\Lambda_4)w_{31}(1)\Big)\Big)=0 \tag{A.4}$$

where

$$\alpha_i=-\frac{1}{3}(4G+(-3F+4G)x_i)(q_i(1)+v(L_i(1)-p^2w_{i1}(1))), \quad i=1,2,3 \tag{A.5}$$

$$\alpha_4=-\frac{1}{3}(3F-4G)p(v-1)(L_4(1)-w_{41}(1)) \tag{A.6}$$

$$\Lambda_i=-\frac{1}{3}\Big(4F+(-3C+4F)x_i\Big)\Big(q_i(1)+v\Big(L_i(1)-p^2w_{i1}(1)\Big)\Big), \quad i=1,2,3 \tag{A.7}$$

$$\Lambda_4=-\frac{1}{3}(3C-4F)p(v-1)\Big(L_4(1)-w_{41}(1)\Big) \tag{A.8}$$

$$q_i(R)=\frac{\partial}{\partial R}L_i(R), \quad i=1,2,3,4 \tag{A.9}$$

Case 3: Soft simply supported circular plates

$$-(\Lambda_4\Psi_3+\Lambda_3\Psi_4)(\alpha_2w_{11}(1)-\alpha_1w_{21}(1))+\alpha_3\Big((\Lambda_4\Psi_2+\Lambda_2\Psi_4)w_{11}(1)-(\Lambda_4\Psi_1+\Lambda_1\Psi_4)w_{21}(1)\Big)+\Big(\alpha_2(\Lambda_4\Psi_1+\Lambda_1\Psi_4)-\alpha_1(\Lambda_4\Psi_2+\Lambda_2\Psi_4)\Big)w_{31}(1)+\alpha_4\Big(\Psi_3(\Lambda_2w_{11}(1)-\Lambda_1w_{21}(1))+\Lambda_3(-\Psi_2w_{11}(1)+\Psi_1w_{21}(1))+(-\Lambda_2\Psi_1+\Lambda_1\Psi_2)w_{31}(1)\Big)=0 \tag{A.10}$$

where

$$\Psi_i=\frac{2}{9}p(-12F+16G+(9C-24F+16G)x_i)(L_i(1)-w_{i1}(1)), \quad i=1,2,3 \tag{A.11}$$

$$\Psi_4=\Big(C-\frac{8}{3}F+\frac{16}{9}G\Big)(L_4(1)-q_4(1)-p^2w_{41}(1)) \tag{A.12}$$

Case 4: Free circular plates

$$\alpha_4(\Lambda_3(\mu_2\Psi_1-\mu_1\Psi_2)+\Lambda_2(-\mu_3\Psi_1+\mu_1\Psi_3)+\Lambda_1(\mu_3\Psi_2-\mu_2\Psi_3))+\alpha_3(\Lambda_4(-\mu_2\Psi_1+\mu_1\Psi_2)+\Lambda_2(\mu_4\Psi_1+\mu_1\Psi_4)-\Lambda_1(\mu_4\Psi_2+\mu_2\Psi_4))+\alpha_2\Big(\Lambda_4(\mu_3\Psi_1-\mu_1\Psi_3)-\Lambda_3(\mu_4\Psi_1+\mu_1\Psi_4)+\Lambda_1(\mu_4\Psi_3+\mu_3\Psi_4)\Big)+\alpha_1(\Lambda_4(-\mu_3\Psi_2+\mu_2\Psi_3)+\Lambda_3(\mu_4\Psi_2+\mu_2\Psi_4)-\Lambda_2(\mu_4\Psi_3+\mu_3\Psi_4))=0 \tag{A.13}$$

where

$$J_1 = \frac{12(1-\nu)}{\delta^4}\left(\frac{\hat{I}_1}{2} - 4\hat{I}_3 + 8\hat{I}_5\right) + \frac{4}{3}\hat{I}_5\beta^2, \quad J_2 = \frac{12(1-\nu)}{\delta^4}\left(\frac{\hat{I}_1}{2} - 4\hat{I}_3 + 8\hat{I}_5\right) - \frac{16}{9}\hat{I}_7\beta^2$$
$$J_3 = \frac{16(3\hat{I}_5 - 4\hat{I}_7)(\nu-2)}{3\delta^2}, \quad J_4 = -\frac{16(3\hat{I}_5 - 4\hat{I}_7)(\nu-1)}{3\delta^2}, \quad J_5 = -\frac{64\hat{I}_7}{3\delta^2}$$
$$J_6 = \frac{64\hat{I}_7(\nu-2)}{3\delta^2}, \quad J_7 = \frac{16(3\hat{I}_5 - 4\hat{I}_7)}{3\delta^2}, \quad J_8 = -\frac{64\hat{I}_7(\nu-3)}{3\delta^2} \tag{A.14}$$

and

$$\mu_i = p^2(J_7 a_i - J_3 a_i - J_8) w_{i1}(1) + (J_1 a_i + J_2 - J_7 a_i p^2 - J_7 a_i - J_4 a_i p^2 - J_6 p^2 - J_5) L_i(1) + (J_7 a_i + J_5)(q_i(1) + s_i(1)), \quad i = 1,2,3 \tag{A.15}$$

$$\mu_4 = p(J_1 - p^2 J_4) w_{41}(1) - p(J_7 + J_3) L_4(1) \tag{A.16}$$

$$s(R) = \frac{\partial}{\partial R} q(R) \tag{A.17}$$

Appendix B. Exact closed-form transverse displacement

By dropping the lengthy mathematical manipulations associated with deriving the explicit closed-form solutions for the transverse displacement $w(R,\Theta)$, we present below only the final relation in terms of R, Θ and δ:

Case 1: Clamped circular plates

$$w(R,\Theta) = \Bigg[-\frac{(-L_3(1)L_4(1)w_{21}(1) + L_2(1)L_4(1)w_{31}(1))}{(x[2]-x[1])L_3(1)w_{11}(1)w_{21}(1) + \Big((x[1]-x[3])L_2(1)w_{11}(1) + (x[3]-x[2])L_1(1)w_{21}(1)\Big)w_{31}(1)} w_{11}(R)$$
$$+ \frac{(-L_3(1)L_4(1)w_{11}(1) + L_1(1)L_4(1)w_{31}(1))}{(x[2]-x[1])L_3(1)w_{11}(1)w_{21}(1) + ((x[1]-x[3])L_2(1)w_{11}(1) + (x[3]-x[2])L_1(1)w_{21}(1))w_{31}(1)} w_{21}(R)$$
$$- \frac{(-L_2(1)L_4(1)w_{11}(1) + L_1(1)L_4(1)w_{21}(1))}{(x[2]-x[1])L_3(1)w_{11}(1)w_{21}(1) + ((x[1]-x[3])L_2(1)w_{11}(1) + (x[3]-x[2])L_1(1)w_{21}(1))w_{31}(1)} w_{31}(R)\Bigg] \cos(p\Theta) \tag{B.1}$$

Case 2: Soft simply supported circular plates

$$w(R,\Theta) = \Bigg[-\frac{\alpha_4\overline{\Psi}_3 w_{21}(1) + \alpha_3\overline{\Psi}_4 w_{21}(1) - \alpha_4\overline{\Psi}_2 w_{31}(1) - \alpha_2\overline{\Psi}_4 w_{31}(1)}{\overline{\Psi}_3(\alpha_1 w_{21} - \alpha_2 w_{11}) + \alpha_3(\overline{\Psi}_2 w_{11} - \overline{\Psi}_1 w_{21}) + w_{31}(1)(\alpha_2\overline{\Psi}_1 - \alpha_1\overline{\Psi}_2)} w_{11}(R)$$
$$+ \frac{\alpha_4\overline{\Psi}_3 w_{11}(1) + \alpha_3\overline{\Psi}_4 w_{11}(1) - \alpha_4\overline{\Psi}_1 w_{31}(1) - \alpha_1\overline{\Psi}_4 w_{31}(1)}{\overline{\Psi}_3(\alpha_1 w_{21} - \alpha_2 w_{11}) + \alpha_3(\overline{\Psi}_2 w_{11} - \overline{\Psi}_1 w_{21}) + w_{31}(1)(\alpha_2\overline{\Psi}_1 - \alpha_1\overline{\Psi}_2)} w_{21}(R)$$
$$- \frac{\alpha_4\overline{\Psi}_2 w_{11}(1) + \alpha_2\overline{\Psi}_4 w_{11}(1) - \alpha_4\overline{\Psi}_1 w_{21}(1) - \alpha_1\overline{\Psi}_4 w_{21}(1)}{\overline{\Psi}_3(\alpha_1 w_{21} - \alpha_2 w_{11}) + \alpha_3(\overline{\Psi}_2 w_{11} - \overline{\Psi}_1 w_{21}) + w_{31}(1)(\alpha_2\overline{\Psi}_1 - \alpha_1\overline{\Psi}_2)} w_{31}(R)\Bigg] \cos(p\Theta) \tag{B.2}$$

where

$$\overline{\Psi}_i = \frac{2}{9}(-12F + 16G + (9C - 24F + 16G)x_i)(L_i(1) - w_{i1}(1)), \quad i = 1,2,3 \tag{B.3}$$

Case 3: Free circular plates

$$w(R,\Theta) = \Bigg[\frac{-\alpha_4\overline{\Psi}_3\mu_2 - \alpha_3\overline{\Psi}_4\mu_2 + \alpha_4\overline{\Psi}_2\mu_3 + \alpha_2\overline{\Psi}_4\mu_3 - \alpha_3\overline{\Psi}_2\mu_4 + \alpha_2\overline{\Psi}_3\mu_4}{\alpha_3\overline{\Psi}_2\mu_1 - \alpha_2\overline{\Psi}_3\mu_1 - \alpha_3\overline{\Psi}_1\mu_2 + \alpha_1\overline{\Psi}_3\mu_2 + \alpha_2\overline{\Psi}_1\mu_3 - \alpha_1\overline{\Psi}_2\mu_3} w_{11}(R)$$
$$- \frac{-\alpha_4\overline{\Psi}_3\mu_1 - \alpha_3\overline{\Psi}_4\mu_1 + \alpha_4\overline{\Psi}_1\mu_3 + \alpha_1\overline{\Psi}_4\mu_3 - \alpha_3\overline{\Psi}_1\mu_4 + \alpha_1\overline{\Psi}_3\mu_4}{\alpha_3\overline{\Psi}_2\mu_1 - \alpha_2\overline{\Psi}_3\mu_1 - \alpha_3\overline{\Psi}_1\mu_2 + \alpha_1\overline{\Psi}_3\mu_2 + \alpha_2\overline{\Psi}_1\mu_3 - \alpha_1\overline{\Psi}_2\mu_3} w_{21}(R)$$
$$- \frac{\alpha_4\overline{\Psi}_2\mu_1 + \alpha_2\overline{\Psi}_4\mu_1 - \alpha_4\overline{\Psi}_1\mu_2 - \alpha_1\overline{\Psi}_4\mu_2 + \alpha_2\overline{\Psi}_1\mu_4 - \alpha_1\overline{\Psi}_2\mu_4}{\alpha_3\overline{\Psi}_2\mu_1 - \alpha_2\overline{\Psi}_3\mu_1 - \alpha_3\overline{\Psi}_1\mu_2 + \alpha_1\overline{\Psi}_3\mu_2 + \alpha_2\overline{\Psi}_1\mu_3 - \alpha_1\overline{\Psi}_2\mu_3} w_{31}(R)\Bigg] \cos(p\Theta) \tag{B.4}$$

References

[1] A.W. Leissa, *Vibration of plates, NASA SP-169*, Office of Technology Utilization, Washington, 1969.
[2] G.N. Weisensel, Natural frequency information for circular and annular plates, *Journal of Sound and Vibration* 133 (1989) 129–134.
[3] K.M. Liew, Y. Xiang, S. Kitipornchai, Research on thick plate vibration: a literature survey, *Journal of Sound and Vibration* 180 (1) (1995) 163–176.
[4] H. Deresiewicz, R.D. Mindlin, Axially symmetric flexural vibrations of a circular disk, *ASME Journal of Applied Mechanics* 49 (1955) 633–638.
[5] S.S. Rao, A.S. Prasad, Natural frequencies of Mindlin circular plates, *Journal of Applied Mechanics* 47 (1980) 652–655.

[6] K.M. Liew, Y. Xiang, C.M. Wang, S. Kitipornchai, Flexural vibration of shear deformable circular and annular plates on ring supports, *Computer Methods in Applied Mechanics and Engineering* 1 (I 0) (1993) 301–315.
[7] K.M. Liew, J.B. Han, Z.M. Xiao, Vibration analysis of circular Mindlin plates using the differential quadrature method, *Journal of Sound and Vibration* 205 (5) (1997) 617–630.
[8] T. Irie, G. Yamada, K. Takagi, Natural frequencies of circular plates, *Journal of Applied Mechanics* 47 (1980) 652–655.
[9] J.M. Whitney, C.T. Sun, A higher order theory for extensional motion of laminated composites, *Journal of Sound and Vibration* 30 (1973) 85–97.
[10] K.H. Lo, R.M. Christensen, E.M. Wu, A high-order theory of plate deformation – part 1: homogeneous plates, *Journal of Applied Mechanics* 44 (1977) 663–668.
[11] T. Kant, Numerical analysis of thick plates, *Computer Methods in Applied Mechanics and Engineering* 31 (1982) 1–18.
[12] A. Bhimaraddi, L.K. Stevens, A higher order theory for free vibration of orthotropic, homogeneous, and laminated rectangular plates, *Journal of Applied Mechanics* 51 (1984) 195–198.
[13] J.N. Reddy, A refined nonlinear theory of plates with transverse shear deformation, *International Journal of Solids and Structures* 20 (1984) 881–896.
[14] N.F. Hanna, A.W. Leissa, A higher order shear deformation theory for the vibration of thick plates, *Journal of Sound and Vibration* 170 (1994) 545–555.
[15] J.N. Reddy, N.D. Phan, Stability and vibration of isotropic, orthotropic and laminated plates according to a higher-order shear deformation theory, *Journal of Sound and Vibration* 98 (1985) 157–170.
[16] J.L. Doong, Vibration and stability of an initially stressed thick plate according to a higher order deformation theory, *Journal of Sound and Vibration* 113 (1987) 425–440.
[17] H. Matsunaga, Free vibration and stability of thick elastic plates subjected to in-plane forces, *International Journal of Solids and Structures* 31 (22) (1994) 3113–3124.
[18] C.M. Wang, C. Wang, K.K. Ang, Vibration of initially stressed Reddy plates on a Winkler–Pasternak foundation, *Journal of Sound and Vibration* 204 (1997) 203–212.
[19] I. Shufrin, M. Eisenberger, Stability and vibration of shear deformable plates—first order and higher order analysis, *International Journal of Solids and Structures* 42 (2005) 1225–1251.
[20] A.J.M. Ferreira, R.C. Batra, C.M.C. Roque, L.F. Qian, R.M.N. Jorge, Natural frequencies of functionally graded plates by a meshless method, *Composite Structure* 75 (1) (2006) 593–600.
[21] L.W. Chen, J.R. Hwang, Vibrations of initially stressed thick circular and annular plates based on a high-order plate theory, *Journal of Sound and Vibration* 122 (1988) 79–95.
[22] L.W. Chen, J.R. Hwang, Finite element analysis of thick annular plates under internal forces, *Computers & Structures* 32 (1989) 63–68.
[23] Sh. Hosseini-Hashemi, M. Es'haghi, H. Rokni Damavandi Taher, An exact analytical solution for freely vibrating piezoelectric coupled circular/annular thick plates using Reddy plate theory, *Composite Structures* 92 (2010) 1333–1351.
[24] S. Srinivas, C.V.J. Rao, A.K. Rao, An exact analysis for vibration of simply-supported homogeneous and laminated thick rectangular plates, *Journal of Sound and Vibration* 12 (1970) 187–199.
[25] H.J. Ding, R.Q. Xu, Exact solutions for free vibrations of transversely isotropic circular plates, *Acta Mechanica Solida Sinica* 13 (2000) 105–111.
[26] C.F. Liu, Y.T. Lee, Finite element analysis of three-dimensional vibrations of thick circular and annular plates, *Journal of Sound and Vibration* 233 (2000) 63–80.
[27] J. So, A.W. Leissa, Three-dimensional vibrations of thick circular and annular plates, *Journal of Sound and Vibration* 209 (1998) 15–41.
[28] K.M. Liew, B. Yang, Three-dimensional elasticity solutions for free vibrations of circular plates: a polynomials-Ritz analysis, *Computer Methods in Applied Mechanics and Engineering* 175 (1999) 189–201.
[29] D. Zhou, F.T.K. Au, Y.K. Cheung, S.H. Lo, Three-dimensional vibration analysis of circular and annular plates via the Chebyshev–Ritz method, *International Journal of Solids and Structures* 40 (2003) 3089–3105.
[30] H. Rokni Damavandi Taher, M. Omidi, A.A. Zadpoor, A.A. Nikooyan, Free vibration of circular and annular plates with variable thickness and different combinations of boundary conditions, *Journal of Sound and Vibration* 296 (2006) 1084–1092.
[31] Sh. Hosseini Hashemi, M. Omidi, H. Rokni Damavandi Taher, The validity range of CPT and Mindlin plate theory in comparison with 3-D vibrational analysis of circular plates on the elastic foundation, *European Journal of Mechanics A/Solids* 28 (2009) 289–304.
[32] Sh. Hosseini Hashemi, H. Rokni Damavandi Taher, M. Omidi, 3-D free vibration analysis of annular plates on Pasternak elastic foundation via *p*-Ritz method, *Journal of Sound and Vibration* 311 (2008) 1114–1140.
[33] M. Dauge, Z. Yosibash, Boundary layer realization in thin elastic three dimensional domains and two-dimensional hierarchic plate models, *International Journal of Solids and Structures* 37 (2000) 2443–2471.